Low-energy proton reactions of astrophysical interest in the $A \sim 90$–100 region

C. Lahiri and G. Gangopadhyay
Department of Physics, University of Calcutta, 92 Acharya Prafulla Chandra Road, Kolkata-700 009, India
(Received 4 August 2012; revised manuscript received 30 August 2012; published 5 October 2012)

Semimicroscopic optical potentials for low-energy proton reactions in the mass 90–100 region have been obtained by folding the density-dependent M3Y interaction with relativistic mean field densities. Certain parameters in the potential have been deduced by comparing calculated results with the data for elastic scattering. Low-energy proton reactions in this mass region have been studied in the formalism with success. Rates of important astrophysical reactions in the mass region have been calculated.

DOI: 10.1103/PhysRevC.86.047601 PACS number(s): 24.10.Ht, 25.40.Cm, 25.40.Lw, 25.40.Kv

The p-process is a common term given to the astrophysical reactions that are involved in the synthesis of heavy elements but do not correspond to the r- or s-processes. It includes reactions such as proton capture, charge exchange, and photodisintegration. The p-process is known to be important for the production of certain so-called p nuclei, which are beyond the ambit of the slow and fast neutron reactions. A p network involves typically 2000 nuclei, and incorporates, again typically, 20 000 reactions and decays. More details may be found in standard textbooks [for example, Illiadis [1]] and reviews [2].

One obvious problem in studying the p-process is that many of the involved nuclei have very short life times and are not available in our terrestrial laboratories for experiment. Though radioactive ion beams have opened a new vista, we are still far away from having the reaction rates at astrophysical energies for all the main reactions involved in the p-process. Thus, theoretical calculations for such rates remain very important for the p-process. For example, Rapp *et al*. have identified a number of reactions that are very important in the p-process [3]. In the mass 90–100 region, the list includes the photodisintegration reactions emitting protons and leading to the products ^{91}Nb, ^{95}Tc, and ^{99}Rh. The rates for these reactions could be obtained from their inverse, i.e., (p,γ) reactions, if the above nuclei were easily available in laboratories.

There have been numerous theoretical calculations of astrophysical rates [4] employing various models. However, very often in the literature, these theoretical rates are varied by factors ranging from 10 to 100 to study their effects [5]. In some earlier works, we calculated the cross sections of various low-energy proton reactions, some of which are involved in the rapid proton processes in the mass 60–80 region [6–8]. The semimicroscopic optical model was employed for calculation of cross sections using densities from theoretical mean field calculations. It is our aim to fix the various parameters and prescriptions in our procedure by fitting available low-energy cross sections for various reactions in a mass region and calculate the rates for various reactions involving protons, which are important in nucleosynthesis. Thus, a more stringent restriction may be imposed on the variation of rates. Some consequences of the above approach in the rapid proton process have already been analyzed [9,10].

The code TALYS1.4 [11] has been used to calculate cross sections and rates in the Hauser-Feshbach formalism. In our earlier works, it was concluded that the Hartree-Fock-Bogoliubov level densities, calculated in TALYS by Hilaire [12], and the $E1$ γ strength functions, calculated by the same approach, fit the results in the mass 60–80 region. In the present calculation we employ these values to extend our calculations to the mass 90 region.

The method followed in the present procedure has been detailed in our earlier publications [6,7] and is not discussed here. The FSUGold [13] Lagrangian density is employed to calculate the nuclear density. Since we need the density as a function of radius, the calculation is performed in the coordinate space. We employ spherical approximation, because most of the nuclei under study are near closed shells for both protons and neutrons and are not strongly deformed. The effective interaction DDM3Y [14], derived from nuclear matter calculation, has been folded with the nuclear densities to obtain the semimicroscopic optical model potentials in the local density approximation.

Since the nuclear density is an important factor in the present formalism, we have studied the charge radii values. The charge radius is the first-order moment of the charge distribution. In Table I, we compare our results for the charge radii $r_{\rm ch}$ with measurements for those nuclei in this mass region which have been involved in the reactions studied later in this work and for which experimental radius information are available. Charge densities have been obtained by folding point proton densities with a Gaussian form factor to incorporate the effect of the finite size of the proton as in our previous work [8]. It is clear that the charge radii are reasonably well produced in our calculation.

We could not find direct experimental values for charge densities. Hence, we have employed the Fourier-Bessel coefficients for densities extracted from electron scattering experiments in de Vries *et al*. [16] to get the charge densities and plotted two examples in Fig. 1. One can see that the theoretical results reasonably agree with experiments. However, the absence of any information on error prevents us from reaching a firm conclusion.

As a first test of the optical model potential, we have looked at elastic proton scattering at low energies. Elastic scattering involves the same incoming and outgoing channel for the optical model and may be taken to provide the simplest test

 ©2012 American Physical Society

TABLE I. Experimental charge radii values compared with calculated results for the nuclei involved in low-energy proton reactions. The experimental values are from the compilation by Angeli [15].

	r_{ch} (fm)			r_{ch} (fm)	
	Theor.	Expt.		Theor.	Expt.
^{89}Y	4.274	4.242	^{94}Mo	4.366	4.352
^{90}Zr	4.297	4.270	^{95}Mo	4.376	4.362
^{92}Zr	4.317	4.306	^{96}Mo	4.387	4.384
^{94}Zr	4.335	4.331	^{98}Mo	4.407	4.409
^{96}Zr	4.356	4.350	^{96}Ru	4.409	4.393
^{92}Mo	4.344	4.316	^{98}Ru	4.431	4.409

to constrain various parameters involved in the calculation. The proton energy relevant to a typical p-process temperature of 1–3 GK for nuclei in this mass region lies between 1 and 4 MeV. However, scattering experiments are very difficult at such low energies, because the cross sections are extremely small, and hence no experimental data are available. We have compared the cross sections at the lowest energies available in the literature with theoretical results.

In Figs. 2 and 3, we present the results of some of our calculations in Zr and Mo isotopes, respectively, along with the corresponding experimental results. Experimental values are from Refs. [17–19] for ^{90,91,92}Zr, and from Ref. [20] for Mo isotopes. To fit the experimental data, the folded DDM3Y potential was multiplied by factors 0.81 and 0.15 to obtain the real and imaginary parts of the optical potential, respectively. Throughout the rest of the work, we use these two factors to obtain the potential. We emphasize that better fits for individual reactions are possible by varying different parameters. But if the present calculation has to be extended to an unknown mass region, this approach is clearly inadequate. Therefore, we have refrained from fitting individual reactions. In our previous work [7,8], we used a different normalization which is in good agreement with experimental values in a wide mass region(A $\approx$ 60–88). But beyond that region, the same set of parameters is unable to fit the experimental data for p nuclei [3] and therefore, we chose the above set of parameters. Though, there are no sharp boundaries for a mass region, for simplicity, we chose it in such a way that a single set of parameters can

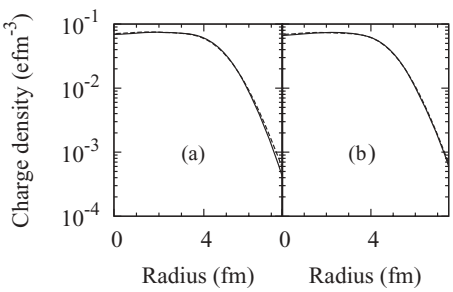

FIG. 1. Comparison of charge density obtained from Fourier-Bessel analysis of experimental electron scattering data (solid line) and calculated in the present work (dashed line) for (a) ^{90}Zr and (b) ^{94}Mo.

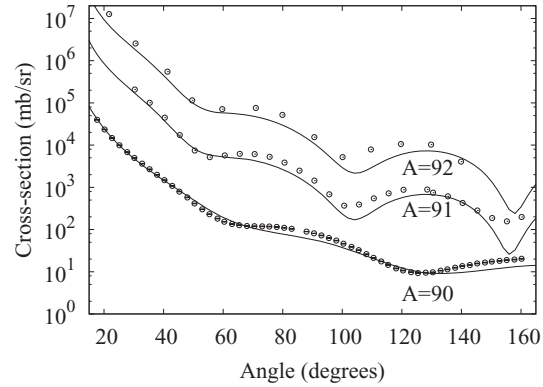

FIG. 2. Experimental and calculated cross sections for elastic proton scattering in Zr isotopes. For $A = 90$, 91, and 92, the proton energies are 9.7, 14.8, and 14.25 MeV, respectively. The cross sections for ^{91,92}Zr have been multiplied by a factor of 100 and 1000, respectively.

fit the entire mass region. In the present work, we chose the mass region $A \approx$ 89–100.

It is clear from Figs. 2 and 3 that the DDM3Y interaction can describe the data well. In fact, we have found that as one goes to lower energies, the quality of agreement tends to improve. Thus at energies relevant to astrophysical interest, we can expect the present method to provide a good description.

The same formalism has been used to study the low-energy (p,γ) reactions in a number of nuclei in this mass region. As the cross section varies very rapidly at low energies, it is more convenient to present the S-factor values. In Figs. 4–7, calculated values are compared with experimental results. Next, we very briefly discuss our results.

For ^{89}Y, the experimental values are from Tsagari *et al.* [21]. For ^{96}Zr, the results are from Chloupek *et al.* [22], though there seems to be certain error in the values in that reference. The numerical values presented there are larger by a factor of 10^3 than the values presented in Fig. 9 of the reference. The latter values appear to be correct to the present authors and are indicated in Fig. 4. The data for Mo and Ru isotopes are from Refs. [23,24], respectively.

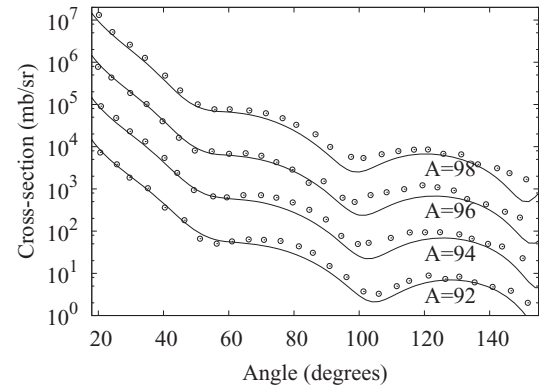

FIG. 3. Experimental and calculated cross sections for elastic proton scattering in Mo isotopes at 15 MeV proton energy. The cross sections for $A = 92$, 94, and 96 have been multiplied by factors of 10, 100, and 1000, respectively.

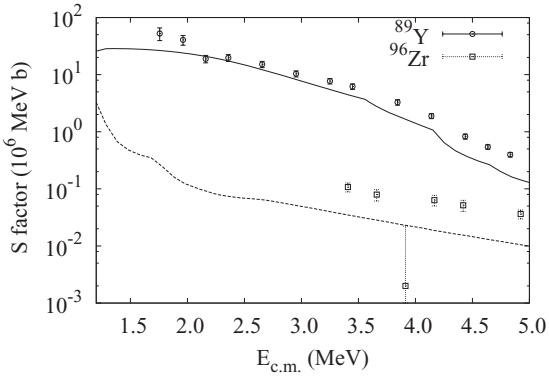

FIG. 4. Experimental and calculated S factors for (p,γ) reactions in ^{89}Y and ^{96}Zr, respectively. The solid (dashed) line indicates calculated results for ^{89}Y(^{96}Zr).

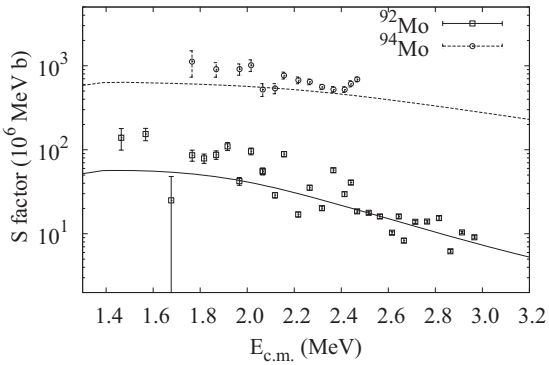

FIG. 5. Experimental and calculated S factors for ^{92,94}Mo(p,γ) reactions. Results for ^{94}Mo have been multiplied by 10. The solid (dashed) line indicates calculated results for ^{92}Mo (^{94}Mo).

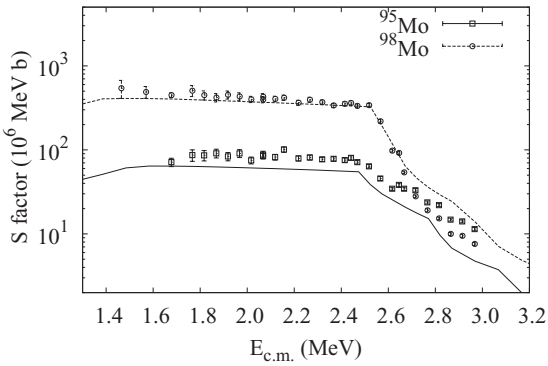

FIG. 6. Experimental and calculated S factors for ^{95,98}Mo(p,γ) reactions. Results for ^{98}Mo have been multiplied by 10. The solid (dashed) line indicates calculated results for ^{95}Mo (^{98}Mo).

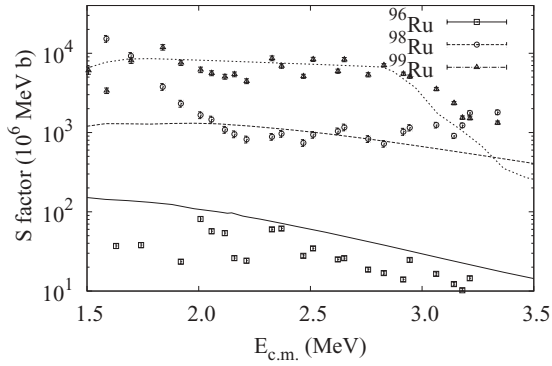

FIG. 7. Experimental and calculated S factors for ^{96,98,99}Ru(p,γ) reactions. Results for ^{98,99}Ru have been multiplied by 10 and 100, respectively. The solid, dashed, and dotted lines indicate results for ^{96,98,99}Ru, respectively.

For the ^{96}Zr target, there are very few experimental points within the energy range important for astrophysical reactions. In ^{89}Y, the trend of the experimental values has been correctly reproduced. For example, at energy 2.36 MeV, S-factor for (p,γ) reaction in ^{89}Y is calculated as 17.87×10^6 MeV b whereas from Ref. [21] it is $19.75(2.68) \times 10^6$ MeV b. None of the experimental values differs by a more than a factor of 2. The last two comments are generally valid for almost all the other reactions. One important exception is the ^{98}Ru(p,γ) reaction, where the measured cross section systematically increases with a decrease in energy below 2 MeV proton energy compared to the calculated values and becomes larger by more than one order of magnitude around 1.6 MeV. It has not been possible to explain such a large increase, which is absent in all low-energy (p,γ) reactions in this mass region for which data are available. In fact, the calculation carried out in Ref. [24], where the experimental values have been published, is also unable to explain such a sudden increase.

We next look for other low-energy reactions involving a proton projectile. The only reaction for which we have been able to find substantial amount of data in the domain of astrophysical energies is the ^{93}Nb(p,n) reaction [25]. Our

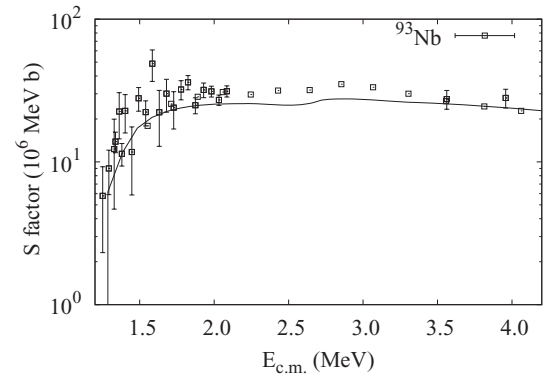

FIG. 8. Experimental and calculated S factors for the ^{93}Nb(p,n) reaction.

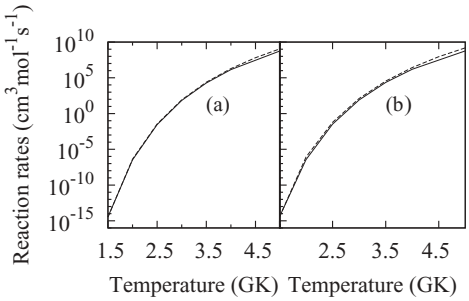

FIG. 9. Comparison of rates (cm^3 mol^{-1} s^{-1}) for (γ, p) reactions from present calculation (solid line) and NON-SMOKER [4] calculation (dotted line) for (a) ^{92}Mo and (b) ^{96}Ru.

results are presented in Fig. 8. One can see that our calculation gives an excellent description of the experimental trends. However, one should also note that the data are rather old and have either very large errors or no quoted error value.

For the sake of completeness, in Fig. 9 we compare the rates of the (γ, p) reaction from the present calculation with rates from the NON-SMOKER [4] calculation for ^{92}Mo and ^{96}Ru. One can see that the present calculation is very similar to the NON-SMOKER values. Therefore, it is expected that all the results can also be reproduced with commonly used NON-SMOKER rates.

From the above discussion, it is possible to conclude that the low-energy reaction cross sections are, except in one case, reasonably reproduced in the above approach. The success in this calculation has enabled us to calculate the astrophysical rates for the reactions identified as important by Rapp *et al*. [3] in the mass 90–100 region. They are presented in Table II.

TABLE II. Rates in cm^3 mole^{-1} s^{-1} for selected (γ, p) reactions of astrophysical importance.

T (GK)	Target		
	^{92}Mo	^{96}Ru	^{100}Pd
1.5	3.45×10^{-15}	3.67×10^{-15}	2.69×10^{-14}
2.0	3.34×10^{-07}	3.64×10^{-07}	1.52×10^{-06}
2.5	2.89×10^{-02}	3.31×10^{-02}	9.85×10^{-02}
3.0	6.77×10^{01}	7.95×10^{01}	1.85×10^{02}
3.5	1.92×10^{04}	2.23×10^{04}	4.30×10^{04}
4.0	1.40×10^{06}	1.57×10^{06}	2.60×10^{06}
5.0	5.87×10^{08}	5.70×10^{08}	7.86×10^{08}

To summarize, relativistic mean field calculation has been performed in nuclei between mass 90 and 100 to obtain the density profiles. They, in turn, have been folded with the density-dependent M3Y interaction to obtain the semimicroscopic optical potential. Parameters in the potential have been fixed by comparing with low-energy proton scattering. Available experimental information on low-energy proton reactions has been compared with theory. Rates of important astrophysical reaction in the mass region have also been calculated.

This work has been carried out with financial assistance of the UGC sponsored DRS Programme of the Department of Physics of the University of Calcutta. C.L. acknowledges support by the UGC. G.G. acknowledges the facilities provided under the ICTP Associateship Programme by ECT*, Trento, where a part of the work has been carried out. Discussion with Alexis Diaz-Torres is gratefully acknowledged.

[1] C. Illiadis, *Nuclear Physics of the Stars* (Wiley-VCH Verlag, Weinheim, Germany, 2007).
[2] M. Arnould and S. Goriely, Phys. Rep. **384**, 1 (2003)
[3] W. Rapp, J. Görres, M. Wiescher, H. Schatz, and F. Käppeler, Astrophys. J. **653**, 474 (2006).
[4] T. Rauscher and F. K. Thielemann, At. Data Nucl. Data Tables **75**, 1 (2000); **79**, 47 (2000).
[5] H. Schatz, Int. J. Mass Spectrom. **251**, 293 (2006).
[6] G. Gangopadhyay, Phys. Rev. C **82**, 027603 (2010).
[7] C. Lahiri and G. Gangopadhyay, Eur. Phys. J. A **47**, 87 (2011).
[8] C. Lahiri and G. Gangopadhyay, Phys. Rev. C **84**, 057601 (2011).
[9] C. Lahiri and G. Gangopadhyay, Int. J. Mod. Phys. E **20**, 2417 (2011).
[10] C. Lahiri and G. Gangopadhyay, Int. J. Mod. Phys. E **21**, 1250074 (2012).
[11] A. J. Koning, S. Hilaire, and M. Duijvestijn, in *Proceedings of the International Conference on Nuclear Data for Science and Technology, April 22-27, 2007, Nice, France*, edited by O. Bersillon, F. Gunsing, E. Bauge, R. Jacqmin, and S. Leray (EDP Sciences, Les Ulis, France, 2008), p. 211.
[12] S. Goriely, S. Hilaire, and A. J. Koning, Phys. Rev. C **78**, 064307 (2008).
[13] B. G. Todd-Rutel and J. Piekarewicz, Phys. Rev. Lett. **95**, 122501 (2005).
[14] G. Bertsch, J. Borysowicz, H. McManus, and W. G. Love, Nucl. Phys. A **284**, 399 (1977); W. D. Myers, *ibid*. **204**, 465 (1973); D. N. Basu, J. Phys. G **30**, B7 (2004).
[15] I. Angeli, At. Data Nucl. Data Tables **87**, 185 (2004).
[16] H. De Vries, C. W. De Jager, and C. De Vries, At. Data Nucl. Data Tables **36**, 495 (1987).
[17] G. W. Greenlees, C. H. Poppe, J. A. Sievers, and D. L. Watson, Phys. Rev. C **3**, 1231 (1971).
[18] L. S. Michelman, S. Fiarman, E. J. Ludwig, and A. B. Robbins, Phys. Rev. **180**, 1114 (1969).
[19] K. Matsuda, H. Nakamura, I. Nonaka, H. Taketani, T. Wada, Y. Awaya, and M. Koike, J. Phys. Soc. Jpn. **22**, 1311 (1967).
[20] H. F. Lutz, D. W. Heikkinen, and W. Bartolini, Phys. Rev. C **4**, 934 (1971).
[21] P. Tsagari, M. Kokkoris, E. Skreti, A. G. Karydas, S. Harissopulos, T. Paradellis, and P. Demetriou, Phys. Rev. C **70**, 015802 (2004).
[22] F. R. Chloupek *et al*., Nucl. Phys. A **652**, 391 (1999).
[23] T. Sauter and F. Käppeler, Phys. Rev. C **55**, 3127 (1997).
[24] J. Bork, H. Schatz, F. Käppeler, and T. Rauscher, Phys. Rev. C **58**, 524 (1998).
[25] C. H. Johnson, A. Galonsky, and J. P. Ulrich, Phys. Rev. **109**, 1243 (1958); C. H. Johnson, C. C. Trail, and A. Galonsky, *ibid*. **136**, B1719 (1964); R. D. Albert, *ibid*. **115**, 925 (1959).